Thermochimica Acta, 230 (1993) 269–292
Elsevier Science Publishers B.V., Amsterdam
SSDI 0040-6031(93)01161-U

Thermal behaviour and thermochemistry of hexachlorozirconates of mononitrogen aromatic bases

Hoan Vu Thanh, Ludwika Gruzdiewa, Janusz Rak and Jerzy Błażejowski *
University of Gdańsk, Department of Chemistry, 80-952 Gdańsk (Poland)

(Received 27 January 1993; accepted 11 March 1993)

Abstract

Thermal features of the hexachlorozirconates of the base (designated B) pyridine, quinoline (isoquinoline) and acridine, as well as several of their methyl substituted derivatives were examined by dynamic and quasi-isothermal–isobaric thermoanalytical methods. These measurements enabled determination of the temperatures of phase transitions, melting and the onset of decomposition. All the compounds undergo dissociation upon increase of temperature, leading to their partial volatilization. It is believed that the primary process, which can be summarized with the equation

$$(BH)_2ZrCl_6(c) \rightarrow 2B(g) + 2HCl(g) + ZrCl_4(ads)$$

is accomplished in several stages, attaining the release of complementary ions from the lattice, formation with these of an intermediate conglomerate loosely bound to the crystal surface and subsequent dissociation of the latter into base, HCl and $ZrCl_4$. Interaction between primarily released molecules was examined at the level of the STO-3G ab inito method considering all electrons and the semiempirical AM1 and PM3 quantum chemistry methods. Decomposition of the compounds is accompanied by side processes affording ZrO_2 and sometimes carbonization products of the organic constituents. The application of the van't Hoff equation to the non-isothermal thermogravimetric curves enabled evaluation of the enthalpies and temperatures of completion of the thermal dissociation. Using values of the former quantity and other thermochemical characteristics available in the literature, the enthalpies of formation and the crystal lattice energies of the compounds were evaluated. The values of the latter quantity were further estimated following the Kapustinskii–Yatsimirskii approach. We tried to reveal relationships between structural, energetic and physicochemical features of the neutral and protonated organic bases, derived by the semiempirical AM1 and PM3 quantum chemistry methods. Furthermore, an attempt was made to correlate the thermal behaviour and thermochemical characteristics of hexachlorozirconates with features of these neutral and protonated base molecules.

INTRODUCTION

Periodic Group IV tetrachlorides have attracted the attention of scientists for a long time owing to their interesting physicochemical features [1–4] and their particularly distinct electron acceptor abilities [1–4]. All the

---

* Corresponding author.

tetrachlorides (M_BCl_4) of the elements of the IVb group (where M_B is C, Si, Ge, Sn or Pb) are non-polar liquids soluble in a number of organic systems [1, 2, 4, 5]. For these reasons M_BCl_4 have been widely used as model compounds when studying intermolecular interactions [1–7]. As a result of such interactions, highly symmetrical octahedral $M_BCl_6^{2-}$ ions result, and these form typical salt-like derivatives [2, 3, 5, 6, 8, 9]. The latter compounds have been the subject of our interest in the past, and in several earlier papers we presented results of the examination of the thermal features and thermochemistry of substances made up of $SnCl_6^{2-}$ [5, 10–13] or $PbCl_6^{2-}$ [14, 15] and numerous organic and inorganic ions, as well as the results of theoretical studies of the crystal lattice energy of several hexahalogenometallates [16–18].

Tetrachlorides of the group IVa elements (M_ACl_4) (where M_A is Ti, Zr or Hf) are much less well characterized, mainly because of the rather diffuse occurrence of the corresponding metals [4]. Selected physicochemical characteristics of M_ACl_4 and other related data are compiled in Table 1. Comparison of Group IVa and IVb derivatives (cf. Table 1 in ref. 5) reveals that the former are more thermally and thermodynamically stable. M_ACl_4

TABLE 1

Selected physical and thermochemical characteristics of halides of the Group IV transition elements at standard pressure

Compound	M.p. [a]/K	B.p./K	Density [b]/ g cm^{-3}	$\Delta_{f,298}H^{\ominus}$ [b,c]/ kJ mol^{-1}	$\Delta_{d(I),298}H^{\ominus}$ [d]/ kJ mol^{-1}	$\Delta_{d(II),298}H^{\ominus}$ [e]/ kJ mol^{-1}	$\Delta_{a,298}H^{\ominus}$ [f]/ kJ mol^{-1}
$TiCl_2$	1308 [2]	1773 [2]	3.13*** [2, 19]	−513.9*** [19]			
				−516.8*** [2]			
$ZrCl_2$	623 (d) [19]		3.6*** [19]	−502.2*** [2, 19]			
$HfCl_2$				−544.1*** [2]			
$TiCl_3$	713 (d) [19]		2.65*** [2, 19]	−721.3*** [2, 19]			
$ZrCl_3$	623 (d) [19]		3.00*** [19]	−749.1*** [2]			
$HfCl_3$				−778.4*** [2]			
$TiCl_4$	248 [19]	410 [2, 4, 19]	1.702** [2]	−763.3* [2, 20]	248†	42†	
	249 [2, 4]		1.726** [19]	−804.6** [2, 19]	289††	83††	
$ZrCl_4$	604(s) [19]		2.803*** [2, 19]	−870.3* [20]	368†	121†	
				−980.8*** [19]	479††	232††	
				−981.4*** [2]			
$HfCl_4$	592(s) [19]			−889* [20]	345†	111†	
				−990.6*** [19]	447††	213††	
				−991.8*** [2]			
$TiCl_6^{2-}$				−1330* [20]			101
$ZrCl_6^{2-}$				−1526* [20]			190
$HfCl_6^{2-}$				−1640* [20]			285

[a] (d) denotes decomposition and (s) indicates sublimation. [b] Asterisks denote gaseous (*), liquid (**) and solid (***) phases. [c] Standard enthalpy of formation. [d] Enthalpy of the reaction $MCl_4(l,s) \rightarrow MCl_2(s) + Cl_2(g)$ (M = Ti, Zr, Hf; $MCl_4(l)$, if M = Ti, and $MCl_4(s)$, when M = Zr, Hf) is marked with two daggers and that of the process $MCl_4(g) \rightarrow MCl_2(s) + Cl_2(g)$ by one dagger. [e] Enthalpy of the reaction $MCl_4(l,s) \rightarrow MCl_3(s) + \frac{1}{2}Cl_2(g)$ (where M = Ti, Zr, Hf; $MCl_4(l)$, if M = Ti, and $MCl_4(s)$, when M = Zr, Hf) is marked with two daggers and that of the process $MCl_4(g) \rightarrow MCl_3(s) + 1/2Cl_2(g)$ by one dagger. [f] Enthalpy of the reaction $MCl_6^{2-}(g) \rightarrow MCl_4(g) + 2Cl^-(g)$; $\Delta_{f,298}H^{\ominus}[Cl^-(g)] = -233.1$ (kJ mol^{-1}) [21].

are solids (if M_A is Zr or Hf) melting at relatively high temperatures. Furthermore, M_ACl_4 and $M_ACl_6^{2-}$ exhibit much lower enthalpies of formation than the analogous derivatives of the group IVb elements [5]. The explanation of these facts arises from the consideration of possible hybridization of the orbitals of the central atom in valence bond terms. The tetrahedral and octahedral hybridization in M_ACl_4 and $M_ACl_6^{2-}$ can (in the first approximation) be represented as $(n-1)d^xnsp^{3-x}$ [22, 23] and $(n-1)d^2nsp^3$ [24, 25], respectively. This means that partially occupied inner shell d orbitals and outer shells s and p orbitals of M_A participate in the formation of molecular orbitals. For comparison, hybridization of the Group IVb elements in the analogous species is best represented as nsp^3 and nsp^3d^2, i.e. hybrids are created predominantly from valence shell orbitals [6, 25, 26]. This results in the former species being energetically favoured.

To reveal how these expected differences in the engagement of the atomic orbitals of a central atom in hexachlorometallate ions influence the thermal and thermochemical stability of salts formed with these, we undertook studies on selected hexachlorozirconate derivatives. This group of compounds was chosen to enable direct comparison of their behaviour with that of hexachlorostannates (Zr and Sn are both fifth row elements) investigated in detail in the past [5, 10–13].

The present paper is devoted to studies on the thermal features and thermochemistry of hexachlorozirconates of mononitrogen aromatic bases. In choosing this group of compounds for investigation, we had in mind that the detachment of two Cl^- ions from MCl_6^{2-}, in addition to decomposition of MCl_4 to form MCl_3 or MCl_2 (Table 1), characterizes relatively high endothermicity, which implies that none of these processes should occur simultaneously. Therefore the investigation of hexachlorozirconates should not cause inconvenience arising from these undesirable side processes.

MATERIALS AND METHODS

Syntheses

All reagents were the best grades available and were purified, where necessary, by standard methods. The hexachlorozirconates were prepared by mixing a solution of $ZrCl_4$ saturated with HCl (Aldrich) in absolute methyl (ethyl) alcohol, with stoichiometric amounts of organic bases dissolved in the same solvent [27, 28]. The precipitates formed were filtered off, carefully washed with anhydrous tetrahydrofuran, and dried in a vacuum desiccator over P_2O_5. The compositions of the compounds were confirmed by determination of the contents of Cl (mercurometric titration of chloride ions) and C, H, N (using a Carlo-Erba elemental analyser, model 1108).

Measurements

The dynamic thermal analyses were carried out on an OD-103 derivatograph (Monicon), with α-Al_2O_3 as reference, in a dynamic nitrogen atmosphere. The samples, weighing 50 mg, were placed in a shallow platinum crucible (cf. ref. 29; Appendix No. 3, crucible No. 2). Other operating conditions were as follows: heating rate $\approx$5 K min^{-1}, sensitivities of DTG, DTA and TG galvanometers 1/10, 1/1–1/5 and 50 mg, respectively.

Thermogravimetric analyses under quasi isothermal–isobaric conditions (Q-mode) [30] were performed on a Q-1500 derivatograph (Monicon) with 50 mg samples placed in a special platinum labyrinth type crucible. The samples were heated at a rate of about 3 or 6 K min^{-1}. The rate of mass loss was adjusted to 2 mg min^{-1}.

Powder diffraction analyses of residues after dynamic and quasi isothermal–isobaric thermal analyses were carried out on a HZG4-A diffractometer (Carl Zeiss, Jena).

The procedure described previously [31] was applied to identify the gaseous products of decomposition of hexachlorozirconates in the presence of oxygen. For this purpose, the sample was placed in a quartz reactor and heated at constant temperature in a stream of air. Organic substances were trapped inside the reactor on a cold finger, whereas more volatile products were carried out of the reactor and absorbed in cyclohexane, an acidified solution of KI or water. The liquid phases thus obtained were checked for the presence of organic molecules chlorine and HCl.

From TG curves, such as those shown in Fig. 1, values of the temperature (T) corresponding to certain values of the apparent extent of reaction (α^*) were derived in the manner described in ref. 14. For each compound examined, a set of α^* vs. T data points was determined on the basis of at least three replicate measurements. An example is given in Table 2.

MO calculations

Geometries of conglomerates possibly created upon interaction of products of the primary thermal dissociation of pyridinium hexachlorozirconate were fully optimized by minimizing the energy with respect to all internal coordinates (without any symmetry constraint), considering all electrons in the ab initio STO-3G method [32, 33] incorporated in HONDO [34] version 8.1. When possible, the optimizations were also performed employing AM1 [35] and PM3 [36] methods. The structures of neutral (B) and protonated (BH^+) base molecules were optimized by the semiempirical AM1 [35] and PM3 [36] methods, incorporated in MOPAC [37] version 6.0. These calculations were carried out using the precise option to provide the strictest convergence criterion [38]. The MOPAC routines were further used

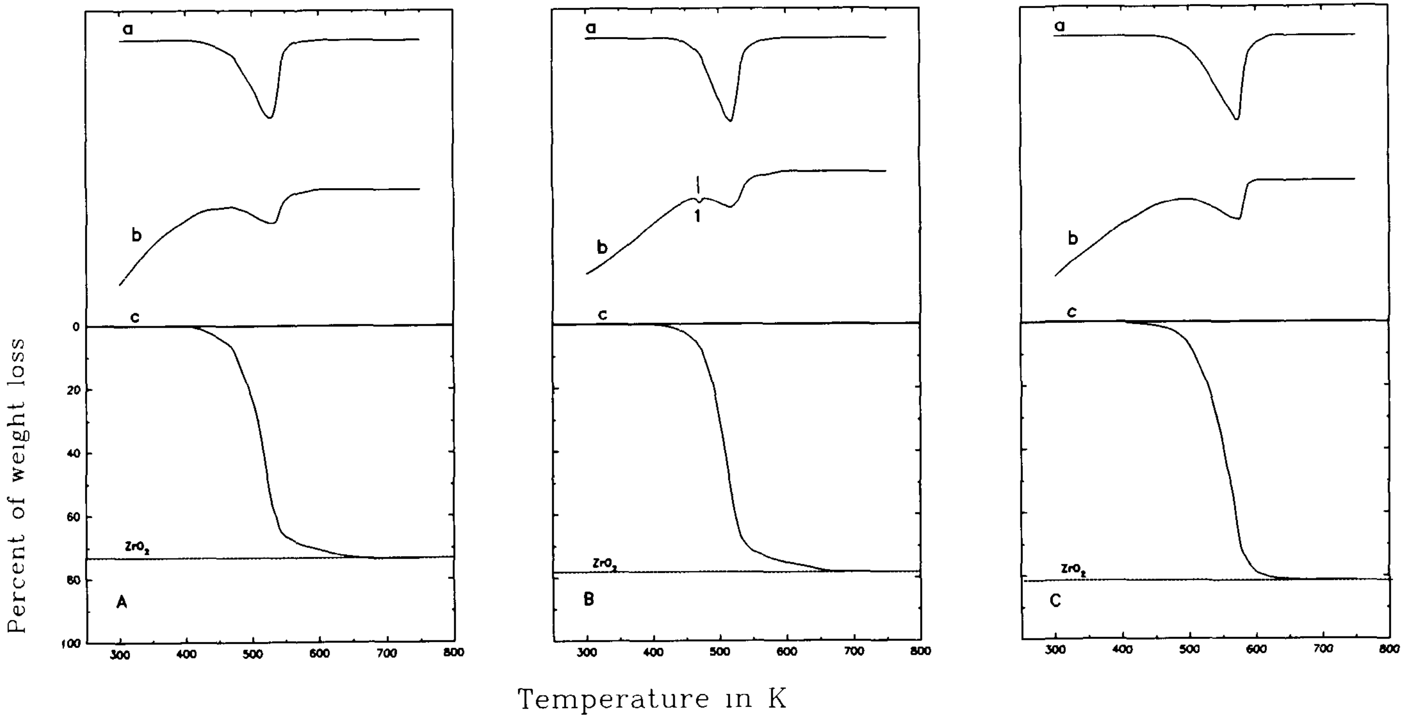

Fig. 1. Thermal analyses of pyridinium (A), isoquinolinium (B) and acridinium (C) hexachlorozirconates carried out in dynamic conditions; a, differential thermogravimetry (DTG); b, differential thermal analysis (DTA); c, thermogravimetry (TG). 1 represents the solid state phase transition. Residues corresponding to ZrO_2 are indicated on the thermogravimetry curves.

TABLE 2

α^* vs. T for the initial stage of volatilization of pyridinium (A), isoquinolinium (B) and acridinium (C) hexachlorozirconates

α^* [a]	T/K		
	A	B	C
0.10	476	473	514
0.18	492	486	529
0.26	504	494	541
0.34	512	501	551
0.42	519	508	559
0.50	526	514	567
0.58	532	520	573
0.66		527	578

[a] Relative to the initial mass of the sample.

to estimate heats of formation, entropies, energies of LUMO and HOMO, energies of orbitals occupied by the lone-pair of electrons (applying procedure localized), as well as charge densities on nitrogen atoms [39, 40] and the lone-pair densities of electrons [41].

Calculations were carried out on a Hewlett-Packard model 730 Apollo work station.

RESULTS AND DISCUSSION

Thermal behaviour of hexachlorozirconates

The results of typical dynamic and quasi isothermal–isobaric thermoanalytical measurements are shown in Figs. 1 and 2. To facilitate discussion

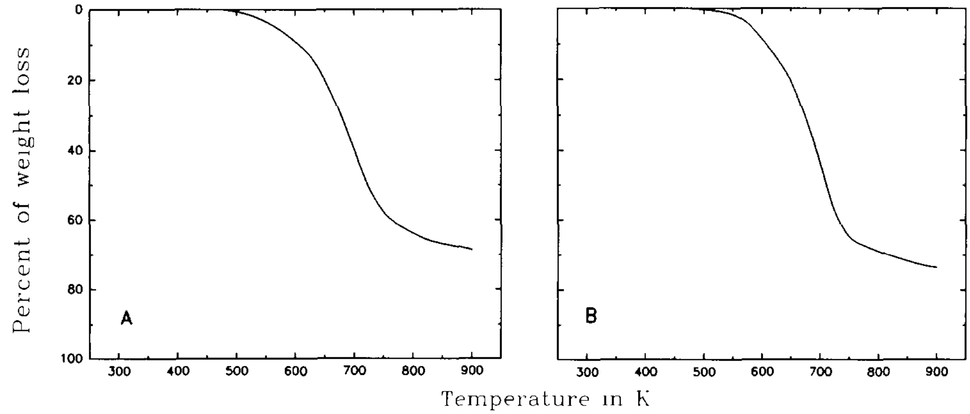

Fig. 2. Quasi isothermal–isobaric analyses of pyridinium (A) and isoquinolinium (B) hexachlorozirconates.

TABLE 3

Thermal characteristics of hexachlorozirconates of nitrogen aromatic bases

No.	Substance[a]	Peak temperature[b]/K				Temperature[b]/K			
		DTG	DTA			$T_{0\,01}$[e]		$T_{0\,1}$[e]	
			T_p	T_σ	T_m	A	B	A	B
1	Pyridine	528	528			418	418	476	475
2	2-Methylpyridine	486			464(d)[c]; 453–463(d)[d]	388	386	445	442
3	3-Methylpyridine	590	582	438[c]	452[c]; 438–448[c]	414	416	505	505
4	4-Methylpyridine	512	512	464(d)[c]	492(d)[c]; 483–493(d)[d]	404	400	457	455
5	2,4-Dimethylpyridine	506	507			417	421	470	469
6	2,6-Dimethylpyridine	564	565			440	437	508	505
7	3,4-Dimethylpyridine	554	554	437[c]		420	425	495	496
8	3,5-Dimethylpyridine	502	502			402	400	453	454
9	2,4,6-Trimethyl-pyridine	532	532			428	429	485	483
10	Quinoline	512	511			415	415	469	467
11	2-Methylquinoline	564	562			454	454	515	513
12	Isoquinoline	514	514	466(d)[c]		425	419	473	471
13	Acridine	576	575			454	540	514	512

[a] Name of organic base. [b] The symbols are taken from ref. 42. T_p, temperature of the peak; T_σ, temperature of the solid state phase transition; T_m, melting temperature; T_α, temperature at which the fraction reacted is equal to α^*. [c] T_m or T_σ determined from DTA curves; (d), decomposition. [d] T_m determined by the standard capillary method; (d), decomposition. [e] A, determined directly from TG curves; B, predicted by approximation of experimental α^* vs. T dependences with eqn. (5).

on the thermal behaviour of hexachlorozirconates, characteristic parameters either derived directly from the thermal analysis curves or evaluated by approximation of thermogravimetric curves with the van't Hoff equation are compiled in Table 3.

In contrast to the hydrochlorides [43] and hexachlorostannates [12] of nitrogen bases examined earlier, none of the hexachlorozirconates studied decomposed with complete volatilization. Solid residues always remained after dynamic (white or slightly grey in colour) and quasi isothermal–isobaric (black in colour) experiments. The amount of solid products in dynamic experiments corresponded exactly to ZrO_2. The presence of the latter compound was confirmed by powder diffraction analysis. On the other hand, ZrO_2 was also found in residues after Q-measurements. A possible explanation of these findings is that the oxygen always present in small amounts in the derivatograph oven reacts with the primarily released $ZrCl_4$, forming ZrO_2. A rough estimate reveals that complete conversion of all the zirconium to ZrO_2 requires only 2.4 and 1.7 cm^3 of oxygen in the case of pyridinium and acridinium hexachlorozirconates, respectively. The colour of the residues is most probably due to carbonization products formed as a result of side processes. In dynamic experiments such processes are negligible and may be facilitated by the formation of non-volatile ZrO_2. The latter covers the surface of the analysed material impeding transfer of organic molecules released upon primary dissociation to the gaseous phase. In quasi isothermal–isobaric measurements, initiation of the decomposition process is moved towards higher temperatures, which creates favourable conditions for the destruction of organic fragments.

In the initial stage of the process, during which more than 60% of the original sample is volatilized, all thermoanalytical curves have the smooth shape (see, for example, Fig. 1) typical of the simple decomposition pattern. It is only at higher temperatures, when volatilization is far advanced, that side processes causing carbonization of organic constituents come to light. For these reasons, the major part of the dynamic thermoanalytical curves may be considered as reflecting simple dissociation of the compounds studied into HCl, base molecules and $ZrCl_4$, accompanied with subsequent oxidation leading to ZrO_2.

Further details are revealed on reviewing the data in Table 3. Decomposition of compounds **3** and **7** is preceded by phase transition and that of compound **3** additionally by melting. Compounds **4** and **12** undergo phase transitions, and **2** and **4** undergo melting, in all cases simultaneously with decomposition. Temperatures characterizing thermal dissociation, i.e. peak maxima on DTA and DTG curves, as well as $T_{0\,01}$ and $T_{0\,1}$, tend to increase upon increase of the molecular mass and size of base molecules. The values of all the above mentioned thermal characteristics are similar to those for hexachlorostannates [12], but are much higher than those for chlorides [43] of the organic bases. Such behaviour may be the consequence of the formally higher thermodynamic stability of $ZrCl_6^{2-}$ and $SnCl_6^{2-}$ salts over that of Cl^- containing salts, as well as the much lower volatility of products of decomposition of both former groups of compounds, i.e. $ZrCl_4$ and $SnCl_4$.

Nature of the decomposition of hexachlorozirconates

The interaction of nitrogen bases with Brønsted acids leads to derivatives which exhibit features typical of ionic substances (see references cited in [43]. This has recently been confirmed by theoretical calculations of the crystal lattice energy of chosen compounds [16–18, 44–46]. Namely, the predicted electrostatic lattice energies, assuming the ionic constitution of the compounds, correlated well with those obtained experimentally. All known features of hexachloroziconates of organic nitrogen bases classify them as ionic substances.

Upon the primary dissociation of salts of nitrogen bases, which can be prompted by increasing the temperature, molecules of organic bases and Brønsted acids or simple decomposition products of the latter (which takes place during dissociation of the compounds studied) are released. Transfer of ions, which it is believed are constituents of crystals of salts of nitrogen bases, to the gaseous phase is neither probable thermodynamically, since it would require much larger amounts of energy than dissociation to neutral molecules, nor has it been confirmed experimentally [47–50]. It must therefore be that ionic fragments in such lattices rearrange before release of products to the gaseous phase in such a way that effective charges on these diminish, causing a decrease of the electrostatic energy of cohesion. As may be expected, this rearrangement is accompanied by proton transfer from a position closer to the basic site to one closer to the acidic site and, sometimes, by changes in the structure of acidic constituents such as facilitate their decomposition (for example, in the case of $ZrCl_6^{2-}$ going to $ZrCl_4$). These processes should not involve substantial changes in the geometry of molecules, and thus overall decomposition should not require the overcoming of an energy barrier higher than the thermodynamic one.

The HCl and base molecules mainly formed upon decomposition tend to evolve into the gaseous phase, since their volatilization temperatures are lower than those of decomposition of the corresponding hexachlorozirconates. $ZrCl_4$ is much less volatile (the literature value for the sublimation temperature is 604 K [4, 8]) and tends to remain in the crucible. This would imply that multistage decomposition could take place, but this has not actually been reflected in thermoanalytical curves. It must therefore be that, simultaneous with the release of $ZrCl_4$ from the lattice, its oxidation occurs, leading to non-volatile ZrO_2, which should follow the equation [9]

$$ZrCl_4(ads) + O_2(g) \rightarrow ZrO_2(c) + 2Cl_2(g) \qquad (1)$$

Taking enthalpies of the formation of $ZrCl_4$(g,c) from Table 1, and assuming for $\Delta_{f,298}H^{\ominus}[ZrO_2(c)]$ a value equal to -1097.7 kJ mol^{-1} [3], it can be shown that oxidation is exothermic by 227.4 or 116.4 kJ mol^{-1} if the substrate is gaseous or crystalline, respectively. The process given by eqn. (1) should therefore be spontaneous from the energetic point of view; it will, however, most probably require the overcoming of some kinetic activation barrier, since earlier studies revealed that oxidation of gaseous $ZrCl_4$ appears to be second order reaction with an activation energy equal to 101.3 kJ mol^{-1} [9]. The occurrence of reaction (1) in dynamic thermoanalytical measurements explains the formation of stoichiometric amounts of ZrO_2. If oxidation ends with reaction (1), then in a stream of gas leaving the reaction zone stoichiometric (to $ZrCl_4$) amounts of Cl_2 should be present. Unfortunately, experiments carried out in a quartz reactor did not confirm this. Actually only HCl was found in the gas stream. It must therefore be that Cl_2 reacts subsequently with organic molecules. This latter problem has been discussed in more detail in one of our earlier papers [31]. The susceptibility of hexachlorozirconates to oxidation has been studied earlier by Denisova et al. [51], whose results confirm our findings.

Taking into account the above considerations, the thermal dissociation of the compounds studied can be schematically presented as a sequence of the following three steps

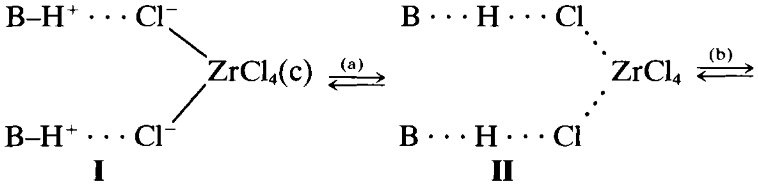

$$\begin{matrix} B\text{–}H^+\cdots Cl^- \\ \qquad\qquad ZrCl_4(c) \\ B\text{–}H^+\cdots Cl^- \end{matrix} \underset{}{\overset{(a)}{\rightleftarrows}} \begin{matrix} B\cdots H\cdots Cl \\ \qquad\qquad ZrCl_4 \\ B\cdots H\cdots Cl \end{matrix} \overset{(b)}{\rightleftarrows}$$

I **II**

$$(2B,\ 2HCl,\ ZrCl_4)(ads) + O_2(g) \overset{(c)}{\rightleftarrows}$$

$$\mathbf{III} \qquad 2B(g) + 2HCl(g) + 2Cl_2(g) + ZrO_2(c) \quad (2)$$

namely (a), rearrangement within the ion triplet (**I**) towards conglomerate **II**, which most probably takes place on the surface of the crystal; (b), dissociation of the conglomerate thus formed towards smaller fragments forming a mobile adsorbed phase (**III**); (c), desorption of products of primary decomposition from the surface accompanied by oxidation leading to ZrO_2 and transport of volatile molecules to the gaseous phase.

The constitution of the ion triplet (**I**) is identical with that in the crystal. Unfortunately, for none of the compounds studied have the solid phase structures so far been established. These can not also be determined theoretically. Therefore, there is no possibility of obtaining an insight into the structure of these species. Attempts to predict the structure and energy of conglomerate **II** were also unsuccessful, as SCF in STO-3G did not converge. On the other hand, the quantum chemistry methods appear useful in examination of the interaction between base, HCl and $ZrCl_4$ molecules either adsorbed on the crystal or subsequently evolved to the gaseous phase. Examples of the most feasible structures of the conglomerates thus formed are demonstrated in Fig. 3, whereas Tables 4 and 5 compile the thermodynamic and structural characteristics of such species determined by two semiempirical (AM1 and PM3) methods and the ab initio method. As can be noticed, HCl and pyridine dimers, as well as the complex of $ZrCl_4\cdots HCl$, are only weakly energetically stabilized. Slightly more energetically stable is the $Py\cdots ZrCl_4\cdots Py$ conglomerate (Fig. 3G). The formation of such species does not, however, seem likely in view of the experimental facts. On the other hand, the entropy factor acts in the opposite direction. This results in stabilization — free enthalpies always

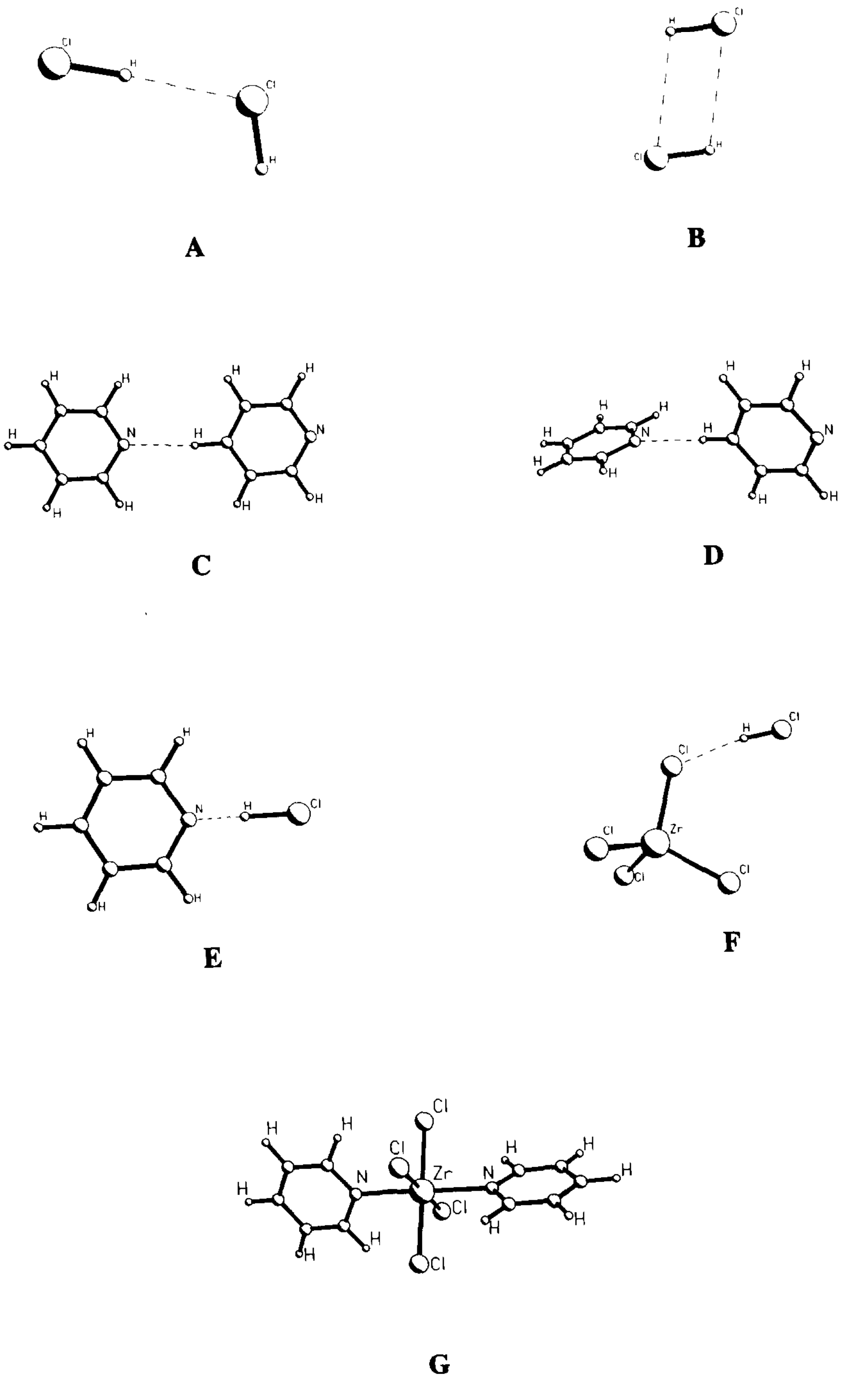

Fig. 3. STO-3G optimized geometries of conglomerates involving products of primary decomposition of pyridinium hexachlorozirconate (hydrogen bonds are indicated by dotted lines).

TABLE 4

Thermochemical quantities for HCl, pyridine (Py) and conglomerates formed by these (see Fig. 3), determined by semiempirical quantum chemistry methods at standard temperature (298 K) and temperature of completion of $(PyH)_2ZrCl_6$ decomposition (540 K)

Species	Method	$\Delta_{f,298}H$/ kJ mol^{-1}	S_{298}/ kJ mol^{-1} K^{-1}	$\Delta_{f,298}G$/ kJ mol^{-1}	$\Delta_{f,540}H$/ kJ mol^{-1}	S_{540}/ J mol^{-1} K^{-1}	$\Delta_{f,540}G$/ kJ mol^{-1}
HCl	AM1	−102.98	186.7	−158.62	−95.92	204.1	−206.13
	PM3	−85.65	186.5	−141.23	−78.58	203.9	−188.69
Py	AM1	134.08	287.5	48.41	159.46	348.2	−28.57
	PM3	127.09	289.7	40.76	153.70	353.4	−37.14
A	AM1	−210.90	316.8	−305.31	−194.90	356.1	−387.19
	PM3	−179.91	303.6	−270.38	−163.97	342.6	−348.97
B	AM1	−211.02	308.5	−302.95	−195.11	347.5	−382.76
	MP3	−177.51	297.8	−266.25	−161.75	336.4	−343.41
D	AM1	264.78	528.9	107.17	319.55	660.0	−36.85
	PM3	251.09	537.1	91.03	308.31	674.1	−55.70
E	AM1	22.39	416.0	−101.58	57.74	501.1	−212.85
	PM3	10.99	361.6	−96.77	46.56	447.1	−194.87

being positive for conglomerates engaging products of primary decomposition released to the gaseous phase. Moreover, the predicted equilibrium constants for the formation of conglomerates are very low in the temperature range in which thermal dissociation occurs. This implies that base and HCl molecules released to the gaseous phase exist predominantly as kinetically free species.

Enthalpy of volatilization of hexachlorozirconates

If, as mentioned, primary dissociation of the compounds studied requires only the overcoming of the thermodynamic energy barrier, then the system should reach equilibrium in a relatively short time. This equilibrium is actually accomplished within species involved in the primary decomposition and thus may be regarded as corresponding to the process

$$(BH)_2ZrCl_6(c) \rightarrow 2HCl(g) + 2B(g) + ZrCl_4(ads) \qquad (3)$$

It can be considered that subsequent oxidation (eqn. (1)) will necessitate substantial structural rearrangements within the $ZrCl_4 \cdots O_2$ activated complex and will require, as mentioned, the overcoming of a substantial kinetic activation barrier, despite the fact that the overall process is exothermic. It therefore seems unlikely that secondary oxidation influences the equilibrium created upon primary decomposition. Having in mind the above considerations, it may be assumed that the experimental extent of decomposition (α^*) is related to $P/P^\ominus$, where P is the equilibrium vapour pressure at a given temperature and $P^\ominus$ is the reference (atmospheric) pressure.

TABLE 5

Structural and thermodynamic characteristics of conglomerates involving products of primary decomposition of pyridinium hexachlorozirconate

Conglomerate (see Fig. 3)	Length of hydrogen bond/Å			Stabilization energy[a] $\Delta_s E$/ kJ mol^{-1}	Stabilization enthalpy[b] $\Delta_{s,298}H$/ kJ mol^{-1}				Stabilization free enthalpy[c] $\Delta_s G$/ kJ mol^{-1}				Equilibrium constant[d] $K_a \times 10^3$			
	STO-3G	AM1	PM3	STO-3G	AM1		PM3		AM1		PM3		AM1		PM3	
					298 K	540 K	298 K	540 K	298 K	540 K	298 K	540 K	298 K	540 K	298 K	540 K
A	2.42	2.41	2.37	−8.085	−4.94	−3.06	−8.61	−6.81	11.93	25.07	12.08	28.41	8.1	3.8	7.6	1.8
B	3.15	2.75	2.63	−4.378	−5.06	−3.27	−6.21	−4.59	14.29	29.5	16.21	33.97	3.1	1.4	1.4	0.52
C	2.43			−6.282												
D	2.65	2.43	2.69	−5.707	−3.38	0.63	−3.09	0.91	10.35	20.29	9.51	18.58	15.3	10.9	21.5	15.9
E	1.35	2.59	1.72	−64.185	−8.71	−5.8	−30.45	−28.58	8.63	21.85	3.70	30.96	30.7	7.7	224.6	1.0
F	2.48			−4.541												
G				−368.196												

[a] $\Delta_s E$ represents the difference between the total energy of the conglomerate and the total energies of its constituent precursors (HCl, pyridine or $ZrCl_4$). [b] $\Delta_{s,298}H$ is the difference between the enthalpy of formation of the conglomerate and the enthalpies of formation of substances (HCl and/or pyridine) taken from Table 4. [c] $\Delta_s G$ represents the difference betwen the free enthalpy of formation of the conglomerate and the free enthalpies of formation of substrates (HCl and/or pyridine) at standard (298 K) and completion of $(PyH)_2ZrCl_6$ decomposition (540 K) temperatures. [d] $K_a = \exp(-\Delta_s G/RT)$; values multiplied by 10^3.

Values of the extent of reaction listed in Table 2 represent a ratio of the mass loss ralative to the initial mass of the sample. They would therefore reflect the degree of conversion in the case of complete volatilization. As, following decomposition of the compounds studied, stoichiometric amounts of ZrO_2 remain in the crucible, all the originally determined α^* must be modified according to

$$\alpha = \alpha^*/\{1 - \mathrm{M}(\mathrm{ZrO_2})/\mathrm{M}[(\mathrm{BH})_2\mathrm{ZrCl_6}]\} \tag{4}$$

where α is the actual extent of decomposition equal to $P/P^\ominus$ and M represents the molecular mass of the species given in parentheses. Taking thus modified values of α and further assuming that the molecules released do not interact, the enthalpy of decomposition ($\Delta_d H^\ominus$) can be evaluated on the basis of the van't Hoff equation [11, 12]

$$\ln \alpha = -\frac{\Delta_d H^\ominus}{4R}\frac{1}{T} + \frac{\Delta_d H^\ominus}{4R}\frac{1}{T_c} \tag{5}$$

where R is the gas constant, the multipland 4 accounts for the fact that primary dissociation of 1 mol of $(BH)_2ZrCl_6$ yields 4 mol of gaseous products (eqn. (3)) and T_c represents the temperature of the completion of decomposition, i.e. the temperature at which P attains $P^\ominus$.

To effect the process as close to the equilibrium state as possible, the analyses were carried out at a moderate heating rate and using as small a sample as possible. Furthermore, the substances were examined in a shallow crucible which enabled distribution of samples over a relatively large surface. These conditions facilitated free diffusion of volatile products and restrained the influence of incidental carbonization.

The values of $\Delta_d H^\ominus$ listed in Table 6 result from eqn. (5) and correspond to reaction (3), i.e. the state where $ZrCl_4$ remains in a condensed phase. For various reasons it is more convenient to present these as standard enthalpies of volatilization ($\Delta_{v,298} H^\ominus$), which reflect the complete transfer of substances to the gaseous phase. This can be done by increasing $\Delta_d H^\ominus$ by the standard enthalpy of sublimation of $ZrCl_4$ ($\Delta_{sub} H^\ominus$), equal to 110.8 kJ mol^{-1} (according to data listed in Table 1). Furthermore, the $\Delta_d H^\ominus$ values refer to the temperature range in which the compounds actually decompose. To enable further considerations it was necessary to modify these so that they refer to 298 K. The overall modification was, therefore

$$\Delta_{v298} H^\ominus = \Delta_d H^\ominus + \Delta_{sub} H^\ominus + \Delta_{fus} H^\ominus + \sum \Delta_\sigma H^\ominus - \int_{298}^{T} \Delta C_p^\ominus \, \mathrm{d}T \tag{6}$$

where $\Delta_{fus} H^\ominus$ is the enthalpy of fusion, the term $\sum \Delta_\sigma H^\ominus$ arises from any

TABLE 6

Thermochemical characteristics for mononitrogen aromatic bases, their cations and hexachlorozirconates at 298 K

Substance, B	B		BH^+		$(BH_2)ZrCl_6$					
	$\Delta_{f,g}H^{\ominus}$/ kJ mol^{-1}	PA^e/ kJ mol^{-1}	$\Delta_{f,g}H^{\ominus\,j}$/ kJ mol^{-1}	r_C^k/ nm	$\Delta_d H^{\ominus\,l}$/ kJ mol^{-1}	$\Delta_{v,298}H^{\ominus}$/ kJ mol^{-1}	T_c/ K	$\Delta_{f,c}H^{\ominus}$/ kJ mol^{-1}	$U^{\ominus}$/kJ mol^{-1} From the thermochemical cycle	From eqn. (10)^m
Pyridine	140.4 ^{a}	928 ^{f,g}	749	0.194* 0.282**	266	354	540	−1128	1093	1251* 1101**
2-Methylpyridine	99.2 ^{a}	937 ^{h}	698		234 (20††)	346	506	−1203	1066	
3-Methylpyridine	106.4 ^{a}	934 ^{h}	709	0.220* 0.267**	181 (5†); (31††)	300	622	−1142	1082	1203* 1124**
4-Methylpyridine	104.1 ^{a}	939 ^{h}	701	0.211* 0.244**	257 (8†); (10††)	366	516	−1213	1082	1219* 1161**
2,4-Dimethylpyridine	63.9 ^{d}	951 ^{h}	649	0.206* 0.292**	318	407	520	−1334	1099	1228* 1087**
2,6-Dimethylpyridine	58.7 ^{a}	956 ^{h}	639		247	331	386	−1269	1014	
3,4-Dimethylpyridine	70.1 ^{d}	951 ^{i}	655	0.197* 0.305**	227 (31†)	343	582	−1258	1035	1246* 1068**
3,5-Dimethylpyridine	72.8 ^{a}	946 ^{h}	663	0.198*	258	349	515	−1258	1051	1244*
2,4,6-Trimethylpyridine	44.7 ^{b}	966 ^{i}	615	0.209* 0.281**	291	378	545	−1344	1041	1223* 1103**
Quinoline	216.7 ^{c}	946 ^{g}	807	0.192* 0.250**	286	375	525	−997	1078	1255* 1151**
2-Methylquinoline	176 ^{d}	968 ^{i}	744	0.194* 0.271**	302	385	580	−1088	1043	1251* 1118**
Isoquinoline	201.7 ^{c}	945 ^{g}	793	0.193*	293 (12†)	394	529	−1046	1099	1253*
Acridine	292.5 ^{c}	968 ^{g}	861	0.188* 0.297**	284	367	586	−837	1026	1263* 1079**

[a] Ref. 52. [b] Ref. 53. [c] Ref. 54. [d] Ref. 12. [e] Proton affinities taken from the literature were corrected relative to the PA value for ammonia of 860 kJ mol^{-1} [55]. [f] Ref. 56. [g] Ref. 57. [h] Ref. 58. [i] Values estimated increasing (in kJ mol^{-1}) by 33 (representing the difference between experimental (Table 6) and AM1 (Table 7) PAs of 3,5-dimethylpyridine), 24 (representing the difference between experimental (Table 6) and AM1 (Table 7) PAs of 2,4- and 2,6-dimethylpyridine) and 22 (representing the difference between experimental (Table 6) and AM1 (Table 7) PAs of quinoline) determined by the AM1 proton affinities of 3,4-dimethylpyridine, 2,4,6-trimethylpyridine and 2-methylquinoline (Table 7), respectively. [j] Values determined on the basis of of eqn. (9) taking heats of formation and proton affinities of base molecules given in the table and heat of formation of the proton equal to 1536.2 kJ mol^{-1} [21, 59]. [k] Values with one asterisk (*) originate from crystal lattices energies of chloride salts [43] and with two asterisks (**) hexachlorostannate salts [12]. They were calculated employing eqn. (10) and assuming $r_{Cl^-} = 0.181$ [62, 63] and $r_{SnCl_6^{2-}} = 0.370$ [10] nm. [l] Heats of phase transitions (†) or melting (††) are given in parentheses. [m] Asterisks indicate r_C values used.

polymorphic transitions which compounds may undergo between 298 K and the onset of the fusion or decomposition process, and $\int_{298}^{T} \Delta C_p^{\ominus}\,\mathrm{d}T$ accounts for the change in enthalpy resulting from changes in the heat capacities of the reactants. Values of $\Delta_{\mathrm{fus}}H^{\ominus}$ and $\Delta_{\sigma}H^{\ominus}$ were estimated by comparison of the areas of DTA peaks relevant to phase transitions with those resulting from the volatilization process and assuming that the latter areas correspond to the $\Delta_{\mathrm{d}}H^{\ominus}$ values listed in Table 6. The estimated quantities are shown in Table 6. The magnitude of $\int_{298}^{T} \Delta C_p^{\ominus}\,\mathrm{d}T$ is difficult to evaluate in the absence of experimental heat capacity data for hexachlorozirconates and their decomposition products. Thus we estimated values of the heat capacity term assuming that $\Delta C_p^{\ominus}$ increases by $15R$ as the result of an increase in the possibilities of the storage of energy in translational and rotational degress of freedom of molecules released to the gaseous phase. The contribution of vibrational degrees of freedom in energy storage is similar and small in both gaseous and solid phases, and can be neglected. Values of $\int_{298}^{T} \Delta C_p^{\ominus}\,\mathrm{d}T$ thus determined amount from −18 to −28 kJ mol^{-1}.

Values of $\Delta_{\mathrm{v},298}H^{\ominus}$ obtained according to eqn. (6) are listed in Table 6.

Thermochemical characteristics of hexachlorozirconates

Various relationships between the thermochemical quantities characterizing the compounds studied are presented in the form of a thermochemical cycle in Scheme 1. All magnitudes in the cycle refer to 298 K and 1 atmosphere. $\Delta_{\mathrm{f}}H$ denotes the enthalpy of formation of a given substance;

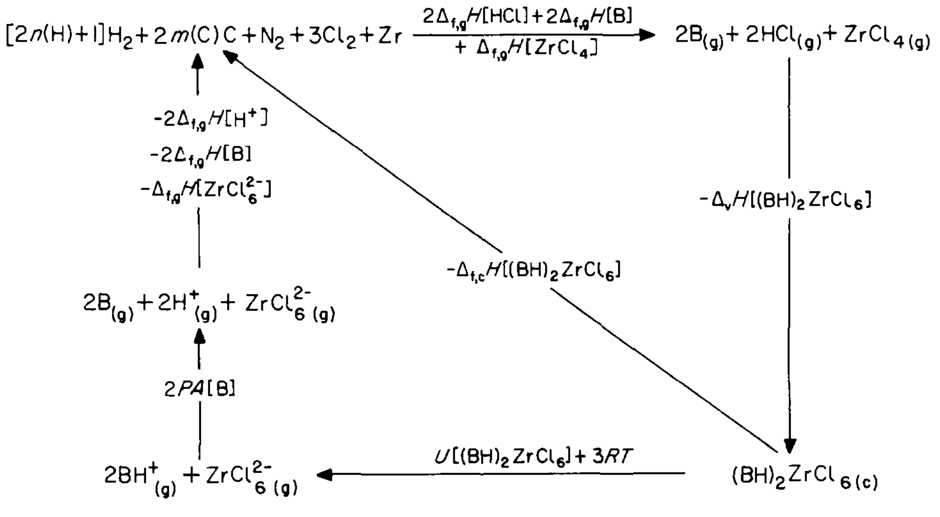

Scheme 1.

$U + 3RT$ is the lattice enthalpy; U represents the lattice energy; PA denotes the proton affinity of the base; $\Delta_v H$ identifies the enthalpy of volatilization; and n(H) and m(C) represent the number of hydrogen and carbon atoms, respectively, in the simplest stoichiometric unit.

The following relationships result from Scheme 1

$$\Delta_{f,c}H^{\ominus}[(BH)_2ZrCl_6] = 2\Delta_{f,g}H^{\ominus}[HCl] + 2\Delta_{f,g}H^{\ominus}[B] + \Delta_{f,g}H^{\ominus}[ZrCl_4] - \Delta_v H^{\ominus}[(BH)_2ZrCl_6] \quad (7)$$

$$U^{\ominus}[(BH)_2ZrCl_6] = 2\Delta_{f,g}H^{\ominus}[BH^+] + \Delta_{f,g}H^{\ominus}[ZrCl_6^{2-}] - \Delta_{f,c}H^{\ominus}[(BH)_2ZrCl_6] - 3RT \quad (8)$$

and

$$\Delta_{f,g}H^{\ominus}[BH^+] = \Delta_{f,g}H^{\ominus}[B] - \Delta_{f,g}H^{\ominus}[H^+] - PA[B] \quad (9)$$

The enthalpies of formation of crystalline hexachlorozirconates and the crystal lattice energies of the compounds are shown in Table 6. To determine these quantities, we used literature values of the enthalpies of formation of the nitrogen bases (Table 6). Proton affinities (PAs) listed in Table 6 were either taken from the literature or estimated using data from the AM1 method. PA values shown in Table 7 were also obtained on the basis of eqn. (9) and using the heats of formation of B and BH^+ predicted by the AM1 and PM3 methods and the experimental value of the heat of formation for the proton (1536.2 kJ mol^{-1}) [21, 59]. Other necessary values for determination of $\Delta_{f,c}H^{\ominus}[(BH)_2ZrCl_6]$ and $U^{\ominus}[(BH)_2ZrCl_6]$ were as follows (in kJ mol^{-1}): $\Delta_{f,g}H^{\ominus}[HCl] = -92.3$ [21], $\Delta_{f,g}H^{\ominus}[ZrCl_4] = -870.3$ [20] and $\Delta_{f,g}H^{\ominus}[ZrCl_6^{2-}] = -1526$ [20].

To shed more light on the crystal lattice energy problems, we further invoked an approximate method developed originally by Kapustinskii [60] and Yatsimirskii [61]. According to these authors, the crystal lattice energy of ionic compounds can be expressed by the equation

$$U/\text{kJ mol}^{-1} = 120.2\frac{(\Sigma n)Z_C Z_A}{r_C + r_A}\left[1 - \frac{0.0345}{r_C + r_A} + 0.087(r_C + r_A)\right] \quad (10)$$

where (Σn) is the total number of ions in the simplest stoichiometric unit of the molecule, Z_C and Z_A denote the numerical values of the charges of cation and anion, respectively, and r_C and r_A are the "thermochemical" ionic radii (in nm). For $r_{ZrCl_6^{2-}}$ a value equal to 0.376 nm, which was obtained from eqn. (10), was assumed using the available data for the crystal lattice energies of alkali metal hexachlorozirconates [20] and the relevant radii of the cations from ref. 63. The lattice energies evaluated on the basis of the Kapustinskii–Yatsimirskii equation are given in the last column of Table 6.

TABLE 7

Energetic, structural and physicochemical features of mononitrogen organic bases (B) and their protonated forms (BH^+) determined theoretically

Compound, B	Quantum chemistry method used	B								BH^+						
		Enthalpy of formation $\Delta_f H$/ kJ mol^{-1}	Proton affinity PA/ kJ mol^{-1}	Energy/eV LUMO	Energy/eV HOMO	Energy of non-bonded orbital/ eV	Lone pair electron density^{c}	Natural net charge at N^{d}	Mulliken net charge at N^{e}	Enthalpy of formation $\Delta_f H$ kJ mol^{-1}	Energy/eV LUMO	Energy/eV HOMO	Natural net charge at N	Mulliken net charge at N	N–H bond length	N–H bond order
Pyridine	AM1	134.1	899.6	0.138	−9.932	−19.366	0.987	−0.139	−0.189	770.7	−5.817	−15.427	−0.081	−0.254	1.008	0.868
		134.3^{a}	900.2^{a}							770.9^{a}						
	PM3	127.1	879.6	−0.004	−10.107	−14.094	0.989	−0.080	−0.099	783.7	−6.093	−15.773	0.533	0.483	0.992	0.968
2-Methylpyridine	AM1	107.3	915.8	0.158	−9.632	−19.263	0.987	−0.143	−0.190	727.7	−5.622	−14.885	−0.092	−0.259	1.007	0.869
		107.6^{a}	916.5^{a}							727.8^{a}						
	PM3	88.5	893.5	0.003	−9.802	−14.020	0.994	−0.077	−0.096	731.2	−5.928	−15.224	0.527	0.458	0.994	0.963
3-Methylpyridine	AM1	100.7	906.5	0.130	−9.632	−19.317	0.986	−0.136	−0.186	730.4	−5.670	−14.827	−0.072	−0.245	1.008	0.869
		100.9^{a}	906.9^{d}							730.7^{a}						
	PM3	87.1	887.9	−0.011	−9.807	−14.036	0.988	−0.075	−0.094	735.4	−5.940	−15.151	0.571	0.502	0.922	0.969
4-Methylpyridine	AM1	101.1	911.9	0.207	−9.888	−19.513	0.987	−0.142	−0.193	725.4	−5.655	−15.296	−0.095	−0.266	1.007	0.870
		101.3^{a}	912.7^{a}							725.3^{a}						
	PM3	86.9	890.5	0.003	−10.060	−14.053	0.989	−0.086	−0.105	732.6	−5.941	−15.339	0.526	0.455	0.992	0.968
2,4-Dimethylpyridine	AM1	74.5	927.3	0.213	−9.589	−19.217	0.987	−0.147	−0.194	683.4	−5.783	−15.113	−0.105	−0.271	1.006	0.871
	PM3	48.5	903.8	0.036	−9.749	−13.983	0.987	−0.084	−0.102	680.9	−5.483	−14.784	0.505	0.435	0.994	0.963
2,6-Dimethylpyridine	AM1	81.5	931.5	0.195	−9.412	−19.160	0.986	−0.148	−0.191	686.2	−5.464	−14.485	−0.103	−0.265	1.007	0.871
	PM3	50.3	906.6	0.043	−9.597	−13.941	0.985	−0.075	−0.092	679.9	−5.774	−14.804	0.508	0.440	0.995	0.958
3,4-Dimethylpyridine	AM1	70.1	917.9	0.188	−9.583	−19.268	0.986	−0.140	−0.190	688.4	−5.526	−14.661	−0.086	−0.257	1.007	0.870
	PM3	49.5	897.9	0.032	−9.726	−14.002	0.988	−0.080	−0.099	687.8	−5.793	−14.832	0.549	0.480	0.992	0.969
3,5-Dimethylpyridine	AM1	67.6	913.0	0.137	−9.434	−19.273	0.986	−0.133	−0.184	690.8	−5.532	−14.544	−0.064	−0.236	1.008	0.870
	PM3	47.3	895.7	0.016	−9.622	−13.988	0.988	−0.070	−0.088	687.8	−5.792	−14.921	0.588	0.522	0.991	0.970
2,4,6-Trimethylpyridine	AM1	48.9	942.3	0.258	−9.374	−19.106	0.987	−0.151	−1.195	642.8	−5.331	−14.388	−0.115	−0.276	1.006	0.872
	PM3	10.4	916.4	0.101	−9.558	−13.909	0.985	−0.080	−0.098	630.2	−5.639	−14.706	0.486	0.417	0.995	0.958
Quinoline	AM1	218.4	924.3	−0.467	−9.178	−19.368	0.986	−0.130	−0.177	830.3	−5.716	−13.696	−0.094	−0.260	1.006	0.871
	PM3	199.0	906.2	−0.647	−9.241	−14.036	0.987	−0.060	−0.077	829.3	−5.928	−13.753	0.530	0.463	0.993	0.964
2-Methylquinoline	AM1	192.6	941.3	−0.415	−9.085	−19.248	0.986	−0.136	−0.180	787.5	−5.538	−13.556	−0.104	−0.264	1.006	0.872
	PM3	160.8	920.7	−0.597	−9.158	−13.950	0.985	−0.060	−0.076	776.3	−5.773	−13.641	0.507	0.441	0.944	0.959
Isoquinoline	AM1	210.0	918.4	−0.557	−9.030	−19.388	0.986	−0.138	−0.189	827.8	−5.603	−13.394	−0.085	−0.256	1.006	0.872
	PM3	197.5	901.4	−0.684	−9.181	−14.090	0.988	−0.080	−0.099	832.3	−5.813	−13.555	0.549	0.481	0.991	0.969
Acridine	AM1	323.0^{b}	957.4	−1.043	−8.575	−19.296	0.985	−0.132	−0.175	901.8^{b}	−5.742	−12.922	−0.131	−0.287	1.004	0.874
	PM3	290.5	936.0	−1.205	−8.609	−13.980	0.985	−0.048	−0.063	890.7	−5.926	−12.912	0.458	0.393	0.995	0.959

[a] Values determined by AM1 from ref 59 [b] Values determined by AM1 from ref 64 [c] For details see ref. 41. [d] Sum of the positive core charge and negative electron density resulting from purely orbital contributions [39]
[e] From Mulliken population analysis [40]

Structure, energetics and physicochemical features of organic bases

As the compounds studied are all made up of the same hexachlorozirconate anion and the protonated molecules of various nitrogen bases, it may be expected that their behaviour and, particularly, their thermal and thermochemical features will be predominantly dependent on the structure and properties of cationic fragments. To reveal how such dependences are represented, it is necessary to know these latter characteristics. Unfortunately, for the relatively large group of organic bases involved in the salts studied, it is difficult to find in the literature a survey of structural, thermochemical, energetic and electronic distribution data. Therefore, to enable a thorough discussion on the above mentioned problems, various structural and physicochemical features for neutral and protonated nitrogen bases applying AM1 and PM3 quantum chemistry methods were predicted. These are compiled in Table 7.

It is generally recognized that salts containing nitrogen bases are formed as the result of hydrogen bonding interactions $(\rangle\mathrm{N{-}H}\cdots(\mathrm{A}))$. The consequence of such interactions is protonation of base molecules, which should in some way be dependent on their proton affinities. Therefore, the knowledge of PAs and factors influencing these may be important in understanding the thermochemistry of the compounds studied. For these reasons, the main emphasis in the discussion below is concentrated on the relationships between PAs and various features of the base molecules.

It is chiefly worth noting that the heats of formation and proton affinities of bases are better reproduced by AM1 than by PM3, which is in accordance with the results of recently published studies [65]. Generally, however, conformity of theoretically predicted and experimental values is not very satisfactory. Nonetheless, careful analysis of heats of formation of neutral and protonated forms enabled the prediction of more reliable values of proton affinities for 3,4-dimethyl- and 2,4,6-trimethylpyridine, and also for 2-methylquinoline (Table 6), than estimated earlier [12, 43].

As proton affinity reflects the ability of molecules for proton attachment, it could be expected to be directly related to the excess of a negative charge imparted to the nitrogen atom (ref. 66 and others cited therein). Net atomic charges on N do not actually show any correlation with predicted proton affinities. It may, however, be noted that the excess of negative charge on the nitrogen of neutral forms is diminished after protonation, which is particularly noticeable when analysing PM3 data. Different dependence is predicted from the Mulliken population analysis in the AM1 method; namely, excess of negative charge at nitrogen increases after protonation.

The next feature which could be considered as corelating with proton affinity would be the density of the lone pair of electrons. Generally, values of this quantity vary only slightly from compound to compound, and differences observed do not follow the tendency of proton affinity changes.

Energies of the LUMO (lowest unoccupied molecular orbital), HOMO (highest occupied molecular orbital) and non-bonded orbital (occupied by a lone pair of electrons) represent the characteristic features of both neutral and protonated forms of nitrogen bases but, unfortunately, do not seem to correlate with proton affinities.

A similar conclusion arises from the analysis of structural characteristics, i.e. bond lengths and orders. Each quantum chemistry method used predicts a characteristic set of data. Comparison of values within a chosen set reveals that these are very similar for all the molecules and small differences do not actually reflect variation of proton affinities.

Examining the data in Table 7 more carefully, further interesting relationships may perhaps also be found.

The above discussion clearly indicates that the PAs of bases actually do not correlate with any of their features chosen for consideration. Nevertheless, data compiled in Table 7 present a unique collection of important physicochemical characteristics for the most representative members of the group of nitrogen aromatic bases, which can be useful in examining many other problems.

Behaviour of hexachlorozirconates versus features constituting these aromatic bases

All nitrogen bases are thermodynamically unstable, since their enthalpies of formation are positive (Tables 6 and 7). This instability increases with an increase in the number of benzene rings in the aromatic system and decreases with an increase in the number of methyl substituents attached to the pyridine aromatic system. The corresponding hexachlorozirconate salts are thermodynamically stable, as their enthalpies of formation are strongly negative (Table 6). In this latter case, trends of stability changes follow those observed for the constituent aromatic bases.

Enthalpies of volatization (Table 6) are very similar for all the compounds studied and do not seem to show any correlation with size, proton affinity or any other feature of organic bases. Values of $\Delta_{v,298}H^{\ominus}$ are, however, generally lower for hexachlorozirconate than for the corresponding hexachlorostannate salts.

Crystal lattice energies do not vary markedly from compound to compound, although they show a downward trend when moving from pyridine to acridine (Table 6). Proton affinities of nitrogen bases tend to increase in the same direction. The relationship between lattice energies and PAs is somewhat unexpected, as an increase in the ability of bases to undergo proton attachment should rather cause the reverse effect. It must therefore be that an increase in dimensions of cationic fragments predominantly causes a decrease of energy of cohesion. This latter statement conforms with several empirical rules [67].

According to eqn. (10), crystal lattice energy may be considered as an additive quantity. This additiveness is reflected through "thermochemical" radii of ions; therefore, using these radii, evaluated on the basis of known crystal lattice energies, the lattice energies of other compounds can be predicted. Such values for the compounds studied are demonstrated in the last column of Table 6. Crystal lattice energies originating from experiment are approximately equal to those predicted by eqn. (10), using "thermochemical" radii for cations evaluated on the basis of the crystal lattice energies of hexachlorostannate salts [12]. Conformity is excellent taking into account that both sets of data were obtained independently. This implies that the additivity rule is roughly obeyed. When "thermochemical" radii of cations originating from chloride salts were used [43], the crystal lattice energies were on average 130 kJ mol^{-1} higher than those resulting from experiments. In the latter case, therefore, the Kapustinskii–Yatsimirskii theory fails. The conclusion which arises from the above considerations is that the Kapustinskii–Yatsimirskii approach applies well to compounds similar in the chemical and structural sense. On the other hand, "thermochemical" radii, being in fact quantities characterizing protonated nitrogen bases, do not show any correlation with their structural and physicochemical features.

CONCLUSIONS

The present paper has provided new information on the thermal behaviour of several simple representative hexachlorozirconates of nitrogen aromatic bases. Moreover, careful analysis of the thermogravimetric curves enabled evaluation of the enthalpies of thermal dissociation and, subsequently, determination of basic thermochemical quantities for the compounds, namely the enthalpies of formation and the crystal lattice energies. It was also revealed that experimental crystal lattice energies of hexachlorozirconate and hexachlorostannate [12] salts of organic bases reproduce each other quite well by the Kapustinskii–Yatsimirskii equation. This paper proves again the usefulness of thermoanalytical methods in studying thermal behaviour and evaluating thermochemical characteristics for solid substances.

A reaction scheme similar to that given by eqn. (2) was originally proposed to explain the mechanism of sublimation of ammonium salts [68–71]. We adopted this idea earlier to account for the dissociation of chlorides [43, 72] and hexachlorostannates [5, 12] of nitrogen bases. Although the scheme demonstrated by eqn. (2) is very similar to that presented in our earlier papers, the meaning ascribed to individual stages is in some sense new.

The qualitative considerations concerning the reaction mechanism were reinforced by the quantum chemistry calculations (semiempirical and at the ab initio STO-3G level), enabling prediction of structures and stabilization energies (enthalpies) of species which may be formed as a result of interactions of primary decomposition products, i.e. HCl, $ZrCl_4$ and base molecules. Moreover, inclusion of entropy changes permitted prediction of free enthalpy changes which accompany such interactions and, consequently, equilibrium constants for the formation of the corresponding conglomerates. The latter considerations revealed that, when released upon thermal dissociation, molecules remain in the gaseous phase as kinetically free species. These findings are quite new and shed a new light on the nature of the thermal dissociation of complex organic ionic substances at the molecular level.

ACKNOWLEDGEMENTS

We thank Mrs. I. Pieńkowska for experimental assistance and Dr. A. Pielak for performing powder diffraction analyses. This work was supported by the Polish State Committee for Scientific Research (KBN) under grant 2 0679 91 01 (contract No. 1156/2/91).

REFERENCES

1 R.J.H. Clark, The Chemistry of Titanium and Vanadium, an Introduction to the Chemistry of the Early Transition Elements (Topics in Inorganic and General Chemistry, Vol. II), Elsevier, New York, 1968.
2 J.C. Bailar, H.J. Emeleus, R. Nyholm and A.F. Trotman-Dickenson (Eds.), Comprehensive Inorganic Chemistry, Pergamon Press, Oxford, 1975, Chapters 16–18, 32 and 33.
3 G. Wilkinson (Ed.), Comprehensive Coordination Chemistry, Vol. 3, Pergamon Press, Oxford, Chapters 26, 31 and 32.
4 N.N. Greenwood and A. Earnshaw, Chemistry of Elements, Pergamon Press, Oxford, 1990.
5 E. Kowalewska and J. Błażejowski, Thermochim. Acta, 101 (1986) 271.
6 J.F. Young, Adv. Inorg. Chem. Radiochem., 11 (1968) 91.
7 J. Błażejowski, Wiad. Chem., 33 (1979) 607.
8 F.A. Cotton and G. Wilkinson, Basic Inorganic Chemistry, Wiley, New York, 1976.
9 E.M. Larsen, Adv. Inorg. Chem. Radiochem., 13 (1970) 1.
10 J. Janiak and J. Błażejowski, Thermochim. Acta, 141 (1989) 93.
11 T. Janiak and J. Błażejowski, Thermochim. Acta, 156 (1989) 27.
12 T. Janiak and J. Błażejowski, Thermochim. Acta, 157 (1990) 137.
13 T. Janiak and J. Błażejowski, J. Therm. Anal., 36 (1990) 2205.
14 J. Błażejowski, J. Szychlinski and K. Windorpska, Thermochim. Acta, 46 (1981) 147.
15 J. Błażejowski, J. Szychlinski and E. Kowalewska, Thermochim. Acta, 108 (1986) 239.
16 P. Dokurno, J. Lubkowski, J. Czerminski and J. Błażejowski, Aust. J. Chem., 44 (1991) 779.
17 P. Dokurno, J. Lubkowski and J. Błażejowski, Pol. J. Chem., 66 (1992) 2047.
18 P. Dokurno, J. Lubkowski and J. Błażejowski, J. Phys. Chem., 97 (1993) 2715.
19 Handbook of Chemistry and Physics, 67th edn., CRC Press, Boca Raton, 1986–1987.
20 H.D.B. Jenkins and K.F. Pratt, Adv. Inorg. Chem. Radiochem., 22 (1979) 1.

21 D.D. Wagman, W.H. Evans, V.B. Parker, R.H. Schumm, I. Halow, S.M. Bailey, K.L. Churney and R.L. Nuttall, J. Phys. Chem. Ref. Data, 11 (1982) Suppl. 2.
22 P.J. Hay and W.R. Wadt, J. Chem. Phys., 82 (1985) 270, 299.
23 R. Kromer and W. Thiel, Chem. Phys. Lett., 189 (1992) 105.
24 H. Basch, A. Viste and H.B. Gray, J. Chem. Phys., 44 (1966) 10.
25 A. Golebiewski, Elementy Mechaniki i Chemii Kwantowej, PWN, Warsaw, 1982.
26 J.C. Bailar (Ed.), The Chemistry of the Coordination Compounds, Reinhold Publishing Corporation, New York, 1956.
27 D.C. Bradley, F.M. Abd-el Halim, E.A. Sadek and W. Wardlaw, J. Chem. Soc., (1952) 2032.
28 R. Beckhaus, U. Dumichen and K.H. Thiele, Z. Chem., 26 (1986) 261.
29 G. Liptay (Ed.), Atlas of Thermoanalytical Curves, Akademiai Kiado, Budapest, 1973.
30 J. Paulik and F. Paulik, Comprehensive Analytical Chemistry, Elsevier, Amsterdam, 1981, Vol. 12, Part A, p. 47.
31 J. Błażejowski and J. Szychlinski, Thermochim. Acta, 35 (1980) 211.
32 W.J. Hehre, R.F. Stewart and J.A. Pople, J. Chem. Phys., 51 (1969) 2657.
33 J.A. Pople, Acc. Chem. Res., 3 (1970) 217.
34 M. Dupuis, in MOTECC-89 (Modern Techniques in Computational Chemistry), S. Chin, E. Clementi, G. Corongiu, M. Dupuis, D. Frye, D. Logan, A. Mohanty and V. Sonnad (Eds.), IBM Corp. 1990, pp. 215–330.
35 M.J.S. Dewar, E.G. Zoebisch, E.F. Healy and J.J.P. Stewart, J. Am. Chem. Soc., 107 (1985) 3902.
36 J.J.P. Stewart, J. Comput. Chem., 10 (1989) 209, 221.
37 J.J.P. Stewart, J. Comput. Aided Mol. Design, 41 (1990) 1.
38 D.R. Boyd, D.W. Smith, J.J.P. Stewart and E. Wimmer, J. Comput. Chem., 9 (1988) 387.
39 J. Sadlej, Obliczeniowe metody chemii kwantowej CNDO, INDO, NDDO, ab initio, PWN, Warsaw, 1988.
40 R.S. Mulliken, J. Chem. Phys., 23 (1955) 1833, 1841, 2338, 2343.
41 P.G. Perkins and J.J.P. Stewart, J. Chem. Soc., Faraday Trans. 2, 78 (1982) 285.
42 R.C. Mackenzie, J. Therm. Anal., 21 (1981) 173.
43 J. Lubkowski and J. Błażejowski, J. Chem. Soc., Faraday Trans. 1, 82 (1986) 3069.
44 J. Lubkowski and J. Błażejowski, J. Phys. Chem., 95 (1991) 2311.
45 J. Lubkowski and J. Błażejowski, J. Chem. Soc., Faraday Trans., 87 (1991) 1333.
46 J. Lubkowski, P. Dokurno and J. Błażejowski, Thermochim. Acta, 176 (1991) 183.
47 P. Goldfinger and G. Verhaegen, J. Chem. Phys., 50 (1969) 1467.
48 C.G. de Kruif, J. Chem. Phys., 77 (1982) 6247.
49 N.S. Golubev and G.S. Denisov, Khim. Fiz., (1982) 563.
50 J.T. Cheung, D.A. Dixon and D.R. Herschbach, J. Phys. Chem., 92 (1988) 2536.
51 T.I. Denisova, L.A. Denisova and A.N. Ketrov, Zh. Neorg. Khim., 19 (1974) 702.
52 J.B. Pedley, R.D. Naylor and S.P. Kirby, Thermochemical Data of Organic Compounds, 2nd edn., Chapman and Hall, London, 1986.
53 Yu. G. Papulov and P.P. Isaev, Zh. Fiz. Khim., 51 (1977) 1405.
54 S.E. Stein and B.D. Barton, Thermochim. Acta, 44 (1981) 265.
55 H.D.B. Jenkins and D.F.C. Morris, J. Chem. Soc., Faraday Trans. 2, 80 (1984) 1167.
56 D.H. Aue, H.M. Webb and M.T. Bowers, J. Am. Chem. Soc., 97 (1975) 4137.
57 M. Moet-Ner (Mautner), J. Am. Chem. Soc., 101 (1979) 2399.
58 E.M. Arnett, B. Chawla, L. Bell, M. Taagepera, W.J. Hehre and R.W. Taft, J. Am. Chem. Soc., 99 (1977) 5729.
59 M.J.S. Dewar and K.M. Dieter, J. Am. Chem. Soc., 108 (1986) 8075.
60 A.F. Kapustinskii, Q. Rev. Chem. Soc., 10 (1956) 283.
61 K.B. Yatsimirskii, Zh. Neorg. Khim., 6 (1961) 518.
62 K.B. Yatsimirskii, Izv. Adad. Nauk SSSR, Otd. Khim. Nauk, (1948) 398.

63 K.P. Mishchenko and A.A. Ravdel, Kratki Spravochnik Fiziko, Khimicheskikh Velichin, 5th edn., Khimiya, Leningrad, 1967.
64 J. Rak, J. Błażejowski and R.J. Zauhar, J. Org. Chem., 57 (1992) 3720.
65 J.L. Ozment and A.M. Schmiedekamp, Int. J. Quantum Chem., 43 (1992) 783.
66 J. Catalan, O. Mo, J.L.G. de Paz, P. Perez, M. Yanez and J. Elguero, J. Org. Chem., 49 (1984) 4379.
67 M.W. Lister, S.C. Nyburg and R.B. Poyntz, J. Chem. Soc. Faraday Trans. 1, 70 (1974) 685.
68 O. Knacke, I.N. Stranski and G. Wolff, Z. Electrochem., 56 (1952) 476.
69 R.F. Chaiken, D.J. Sibbett, J.E. Sutherland, D.K. Van de Mark and A. Wheeler, J. Chem. Phys., 37 (1962) 2311.
70 P.W.M. Jacobs and A. Russell-Jones, J. Phys. Chem., 72 (1968) 202.
71 H.-H. Virnich and A. Hopfner, Ber. Bunsenges. Phys. Chem., 84 (1980) 716.
72 J. Błażejowski, Thermochim. Acta, 68 (1983) 233.